Journal of Civil, Construction and Environmental Engineering
2025, Vol. 10, No. 1, pp. 16-26
https://doi.org/10.11648/j.jccee.20251001.12

Research Article

New Energy Loss Expression for Stepped Spillways with Channel Slopes 26.6° and Below

Okechukwu Ozueigbo*, Jonah Agunwamba

Department of Civil Engineering, University of Nigeria, Nsukka, Nigeria

Abstract

A stepped spillway is a hydraulic structure built at storage and detention dams to discharge flood water that cannot be safely kept in the reservoir. It was created to minimize the kinetic energy that would have otherwise produced dangerous scour at the natural river bed beneath the spillway. They discharge this energy in floodwater using their stepping nature. Several studies show the detrimental consequences of falling water's kinetic energy on the river bed underneath the structure. Only a handful of these studies, however, have evaluated the impact of energy losses caused by stepped spillways with channel slopes 26.6 °or less. As a result, there are gaps in the rules and recommendations for designers of stepped spillways with channel slopes below 26.6 °. Furthermore, the existing models for forecasting energy dissipation in stepped spillways for channels of all slopes include a parameter, the friction factor, f, which is difficult to estimate with precision, leading to its subjective estimation by those involved in the stepped spillway design. The goal of this study is not only to provide designers with design recommendations and information for stepped spillways with channel slopes below 26.6 °, but also to eliminate the 'troublesome' frictional factor; f. Using phase-detection intrusive probes, air-water flow tests were carried out in nappe, transitional, and skimming flows on a stepped spillway with channel slope below 26.6 ° in a large facility. New expressions for evaluating energy losses in stepped spillways with slopes 26.6 ° or less are developed. Regarding energy dissipation, the data from the latest models compare well with the measured data, with high coefficients of correlation that range between 0.95 and 0.99. All of the measured data and the estimated data are in good agreement. The models are simple to use.

Keywords

Stepped Spillway, Energy Dissipation, Nappe Flow, Skimming Flow

1. Introduction

Many scholars have conducted investigations and developed equations that govern Nappe flow, Transition, and Skimming flow regimes in stepped spillways, including [9, 18, 20, 34].

Many of these equations still need to be verified by researchers, while some have already been confirmed. These researchers looked into and tried to find the ideal design and configuration of steps to maximize energy dissipation and decrease basin sizes.

The effect of step geometry on energy dissipation in the stepped spillway has not been extensively studied by scholars. In this field, there is a knowledge deficit.

Therefore, this study is conducted in an effort to offer some

*Corresponding author: ozueigbo.okechukwu.pg78995@unn.edu.ng (Okechukwu Ozueigbo)

Received: 14 October 2024; **Accepted:** 13 November 2024; **Published:** 22 January 2025

knowledge in that field.

If floodwater's energy, particularly its kinetic energy, is not securely dispersed, significant harm could result. One kind of device used to release floodwaters is the stepped spillway. It is made up of an open channel and several drips that are inverted. These drops present high flow impediment, which causes energy loss. Due to this energy loss, smaller and more cost-effective dissipation structures are designed downstream of the chute.

A critical point at which air would be entrained in the flow would be achieved as the discharge down the spillway was raised.

Two-phase flow or air-water flow is the term used to describe this phenomenon.

Chanson and Stephenson [18, 34] classified the flow over the stepped spillway based on experimental observations into three different flow regimes:

a) Nappe flow regime or jet flow regime for lower discharges;
b) Transition flow for medium discharges; and
c) Skimming flow regime for higher discharges.

1.1. Nappe Flow

Similarly, Peyras et al [30] identified two types of nappe flow: flow with a fully developed hydraulic jump for low discharge and small flow depth, and flow with a partially developed hydraulic jump. In the nappe flow regime, a sequence of freely falling water flows down from one step to the next lower step with the development of a hydraulic jump at each step. This type of flow can be likened to a sequence of separate drop structures linked together [9, 16]. It flows from each step and passes through critical depth at the brink of the step forming a supercritical free-falling jet and returning to subcritical flow downstream of the jump. The flow hits the step below as a freely falling jet, with the energy dissipation occurring by a jet breakup in air, by jet mixing on the step, and by the formation of a fully developed or partial hydraulic jump on the step.

For nappe flow to occur, the step horizontal tread needs to be greater than the water depth [34]. In dam design, this would result in a relatively flat slope. The step height, h, must be large for nappe flow to occur. This situation may apply to relatively flat stepped channels or at low flow rates.

According to Peyras et al [30] the step height needs to be at least two or three times the critical flow depth and the tread of the steps needs to be two or three times the step height.

The slopes of these reaches were such that a hydraulic jump occurred at the base of each drop.

If the length of the drop added to the length of the roller, Lr, is less than the length of the horizontal step, l, a fully developed hydraulic jump can take place (Figure 1). Chanson [10] states that a fully developed nappe flow with a fully developed hydraulic jump occurs for discharges smaller than a critical value defined by:

$$\left(\frac{d_c}{h}\right)_{char} = 0.0916\left(\frac{h}{l}\right)^{-1.276} \quad (1)$$

Where the correlation - Eq (1) - is valid for $0.2 \leq h/l \leq 6$
Where l is the step length.
Nappe flow for a fully developed hydraulic jump occurs for

$$\tan\theta = {}^{h}/_{l} < 0.2 \quad (2)$$

Several dams in South Africa were built with stepped spillways. Stephenson [34], from his experience, suggested that the most suitable conditions for nappe flow situations are:

$$\tan \propto = {}^{h}/_{l} < 0.2$$

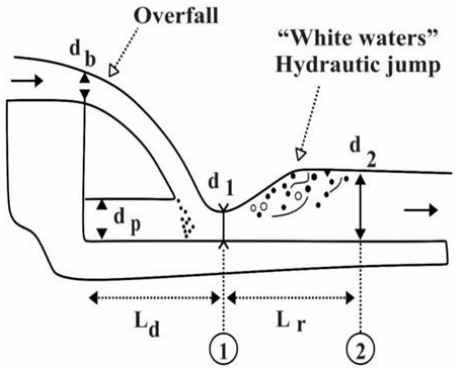

Figure 1. *Nappe flow regime (Flow at a drop structure).*

Energy Dissipation

In a nappe flow regime with a fully developed hydraulic jump, the head loss at any intermediate step equates the energy loss. The total head loss, ΔH, along the spillway equals the maximum head available, H_{max}, and the residual heat, H_1, at the bottom of the spillway [11].

$$\frac{\Delta H}{H_{max}} = 1 - \frac{\frac{d_1}{d_c} + \frac{1}{2}\left(\frac{d_c}{d_1}\right)^2}{\frac{3}{2} + \frac{H_{dam}}{d_c}} \; ungated\ spillway \quad (3)$$

$$\frac{\Delta H}{H_{max}} = 1 - \frac{\frac{d_1}{d_c} + \frac{1}{2}\left(\frac{d_c}{d_1}\right)^2}{\frac{H_{max}+H_0}{d_c}} \; gated\ spillway \quad (4)$$

Where H_{dam} is the dam height and H_0 is the reservoir free-surface elevation above the spillway crest. The residual energy is dissipated at the toe of the spillway by a hydraulic jump in the dissipation basin.

1.2. Partial Nappe Flow

In this type of flow, the nappe does not fully impinge on the step surface and it disperses with considerable turbulence. The flow is supercritical down the length of the spillway. For a given step geometry, an increase in flow rate may lead to an

intermediate flow pattern between nappe and skimming flow - the transition flow regime is also called a partial nappe flow. The transition flow is characterized by a pool of circulating water and is often accompanied by a small air bubble (cavity), significant water spray, and the deflection of the water jet immediately downstream of the stagnation point (Figure 2). The transition flow pattern exhibits significant longitudinal variations of the flow properties on each step. It does not present the coherent appearance of skimming flows. The transition from one type of flow to another is gradual and continuous. As a result, both the nappe flow and the skimming flow appear simultaneously in a certain range, one of them on some steps and the other on the remaining, both changing spatially and temporarily.

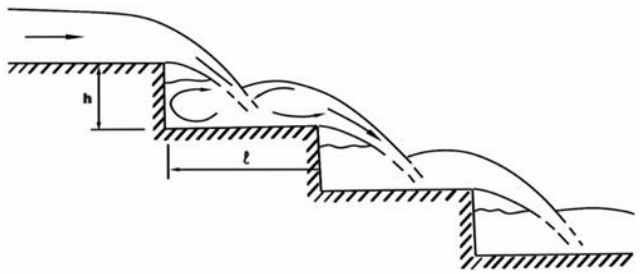

Figure 2. *Nappe flow with partially developed hydraulic jump.*

1.3. Skimming Regime

In skimming flow, the water flows down the stepped face as a coherent stream. It skims over the steps and is supported by the recirculating fluid trapped between them. The external edges of the steps form a pseudo bottom over which the flow skims. Beneath this bottom, recirculating vortices are formed, which are sustained by the transmission of shear stress from the water flowing past the edge of the steps. At the upstream end, the flow is transparent and has a glossy appearance and no air entrainment takes place. After a few steps, the flow is characterized by air entrainment similar to a self-aerated flow down a smooth inverted spillway. There is a continuous exchange of flow between the top layer and vortices formed on steps. The flow rotates in the vortex for a brief period and then returns to the main flow to proceed on down the spillway face. These vortices are supported through the transmission of shear stress from the fluid flowing past the edges of the steps (Figure 4). Chanson [14] states that in addition to this, small vortices are generated continuously at the corner of the steps. It occurs with the submergence of the steps with the development of a fully aerated uniform flow downstream of a long chute. Along the upstream steps, a non-aerated flow region exists in which a turbulent boundary layer develops. Air entrainment in the flow begins where the boundary layer intersects the free surface, referred to as the point of inception. Downstream of the point of inception, the flow continues to aerate and varies gradually in depth (Figure 3). The flow eventually becomes a fully aerated uniform flow in which the water depth, velocity, and air concentration become constant [3, 10] (Figure 4).

The condition is very difficult to establish analytically. Therefore, empirical equations have been proposed by many investigators for the delineation of the skimming flow from nappe flow over the stepped spillway. Essery and Horner [20, 26] reported that it is very difficult to distinguish between nappe and skimming flow for flatter slopes having $< 0.4\,{}^{S_h}/_{l}$

It must be noted that the data of Peyras et al. [27, 30] were obtained on a gabion stepped spillway model. The infiltration through the gabion is likely to affect the flow conditions and may explain smaller values of $(dc/h)_{onset}$ than for [32, 33].

Chanson [18, 21, 24] stated that energy dissipation occurs by momentum transfer, or the transmission of turbulent shear stress, between the skimming stream and the vortices.

Many of the researches on the stepped spillway skimming flow has concentrated on determining the profile of the turbulent boundary layer, the location of the point of inception, and the concentration of air in the flow. All of these factors influence the design of stepped spillways. Specifically, knowledge of the concentration and distribution of aeration is important in determining the water depth, velocity, and hence the amount of energy dissipation along the slope [24].

Numerous researchers have observed and analyzed the flow regime change from Nappe to Skimming in a spillway and linked the parameters, which have been related to flow critical depth, d_c, and the spillway shape, which are the non-dimensional ratios dc /h and h/ l [5, 6, 25].

Chanson, Rajaratnam [7, 8, 31] took into account these non-dimensional parameters dc /h and h/ l. He proposed that values of dc/ h > 0.8 will produce skimming flow in the range of $0.42 \leq h/l \leq 0.842$ of the skimming, leaving the nappe flow regime when flow dc/ h < 0.8 whatever the geometric specifications of the structure might be.

Studies have, however, shown that the majority of the changes in flow regime occur for the flow rate, dc/h, less than this proposed 0.8.

For small discharges and flat slopes, the flow regime is the nappe flow regime. An increase in discharge or channel slope may induce the appearance of a skimming flow regime.

Chanson [18] in his result, also took into account the analysis of Beitz and Lawless, Degoutte et al, Essery and Horner [1, 19, 20] proposed that the skimming flow regime occurs for discharges larger than a critical value defined as:

$$(d_c)_{onset}/h = 1.06 - 0.465\ h/l \qquad (5)$$

Where $(d_c)_{onset}$ is the characteristic critical depth.

Chanson [8] stated that skimming flows occur when $d_c/h > (dc/h)_{onset}$

He noted that Eq (5) was deduced for h/l that ranges from 0.2 to 1.3 and that further experimental work is required to verify or modify the equation outside the range.

Several researchers have published works on the impact, of

scale effects in modeling stepped spillways [2, 4, 15, 23, 31].

The scale effect is the slight misrepresentations, which occur when secondary forces like viscous forces and surface tension forces in turbulent flow are ignored. It is overlooked in many open-channel flows. However, if they are ignored in highly air-entrained flows in stepped spillways, where they play significant roles, they could lead to scale effects and wrong interpretations of results [2]. Scale effects in stepped spillway models are likely to occur with scales lower than 10: 1, Reynolds number smaller than 1×10^5, Weber number smaller than 100, and step heights lesser than 3 cm.

Energy Dissipation

The energy dissipated occurred to keep stable depression vortices. If uniform flow conditions are reached downstream of the spillway, the energy loss could be calculated as follows [10] (Figure 4):

$$\frac{\Delta H}{H_{max}} = 1 - \frac{\left(\frac{d_w}{d_c}\right)\cos\theta + \frac{1}{2}\left(\frac{d_c}{d_w}\right)^2}{\frac{H_{dam}}{d_c} + \frac{3}{2}} \quad (6)$$

Where d_w is the clear water depth, U_{avg} is the average velocity, the total head loss may be rewritten in terms of the friction factor, f, the spillway slope, θ, in degree, the critical depth, dc, and the dam height, H_{dam}:

$$\frac{\Delta H}{H_{max}} = 1 - \frac{\left(\frac{f}{8sin\theta}\right)^{1/3} cos\theta + \frac{E}{2}\left(\frac{f}{8sin\theta}\right)^{-2/3}}{\frac{H_{dam}}{d_c} + \frac{3}{2}} \quad (7)$$

Eq (6) computed for spillway slope with θ = 52 (degrees) and friction factor, f = 0.3 and f = 1.30 represented average flow resistance on smooth spillways and stepped spillways, respectively. where E is the kinetic energy correction coefficient, θ is the dam slope in degrees.

$$\frac{\Delta H}{H_{max}} = \left[0.049\frac{Nh}{d_c}\right]^{0.353} N^{0.06} h^{0.124} \theta^{-0.157} \quad (8)$$

Eq (8) is developed for skimming flow when spillway slope is between 26.6 ° and 21.8 °, h (cm) is not more than 20, N is not more than 20, and dc/h is between 1.0 and 3.7 [29].

$$\frac{\Delta H}{H_{max}} = \left[0.029\frac{Nh}{d_c}\right]^{0.353} N^{0.06} h^{0.124} \theta^{-0.157} \quad (9)$$

Eq (9) is developed for skimming flow when h (cm) is not more than 20, N is not more than 20, θ (degrees) is between 21.8 ° and 3.4 °, and dc/h is between 1.0 and 3.6 [29].

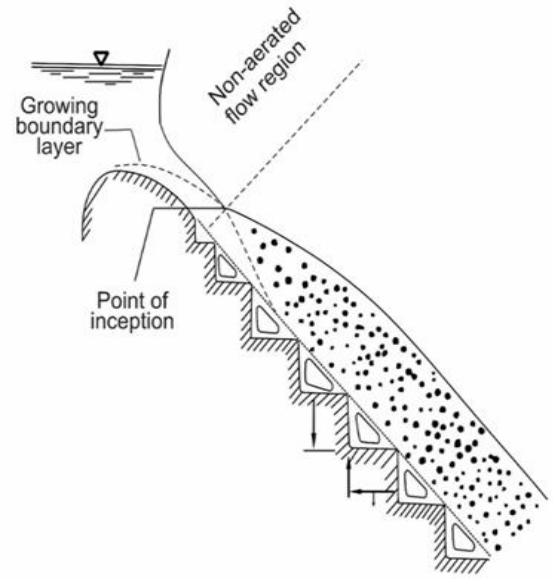

Figure 3. *Skimming flow regime - Sorensen [32].*

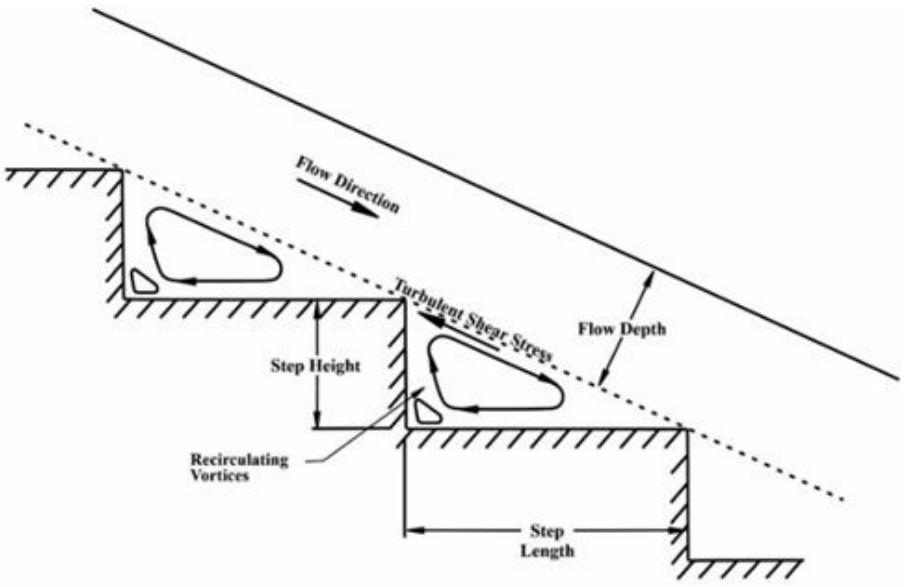

Figure 4. *Skimming flow regime with uniform flow conditions.*

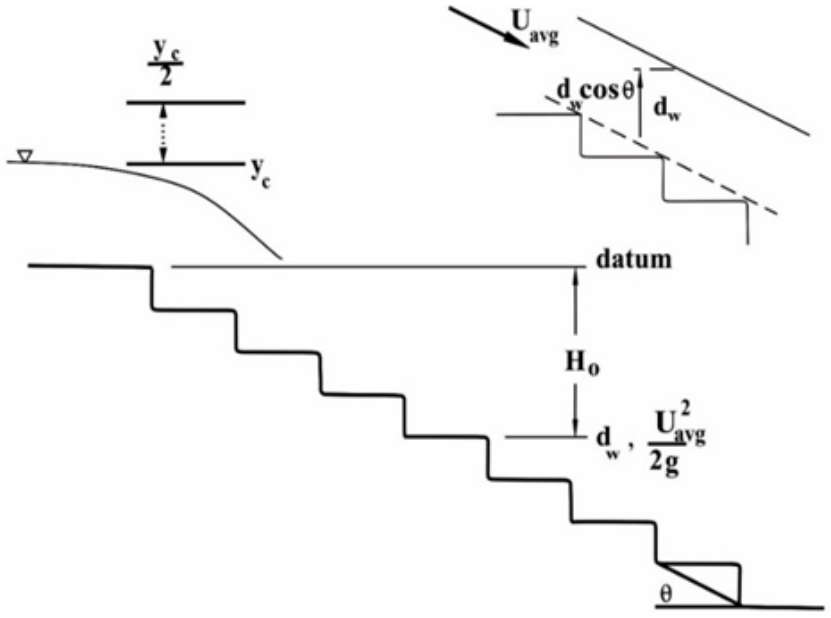

Figure 5. *Arrangement of the spillway with the definition of the variables.*

2. Material and Methods

The authors carefully selected eleven publications on horizontal stepped spillways with minimum step heights of 3 cm, undistorted Froude values, and large dimensionless discharges corresponding to Reynolds numbers between 1×10^5 and 1×10^6.

These researchers used experimental facilities on large scale to minimize scale effects that affect the air-water flow processes in high-velocity free-surface flows [23]. They measured air-water flow properties at all step edges downstream of the inception point of air-entrainment with conductivity phase-detection intrusive probes and optical fiber probes.

Use of a Dall Tube flow meter, or V-notch for flow rates, Prandtl-Pitot for flow velocities, or point gauge for clear water flow depth to obtain air-water flows properties is not practicable as large quantities of air are entrained at the air-water interface [11, 12].

The principle of the conductivity probe is based on the difference between the resistivity of air and water, which provides an instantaneous voltage signal [13, 17]. The threshold technique analyzes signals - from a single sensor - used to calculate a) the time-averaged local air concentration or void fraction C, b) the number of air-to-water (or water-to-air) voltage changes expressed as bubble count rate F, and c) the air bubble and water droplet chord sizes. For a double-tip conductivity probe with longitudinal separation between the two probe sensors, the cross-correlation analysis of the signals leads to the local time-averaged interfacial velocity V [10].

Details about the signal processing techniques could be found in [16, 22].

The double-tip conductivity probes used had sensor sizes of Ø = 0.13 mm and 0.25 mm and were sampled for a period of 45 s with a frequency of 20 kHz per sensor.

The discharges comprised transition and skimming flow rates of $0.035 \leq q_w \leq 0.234$ m^2/s for the spillways with $\theta = 8.9°$ and $0.02 \leq q_w \leq 0.249$ m^2/s and for $\theta = 26.6°$, Reynolds numbers of $1.4 \times 10^5 \leq Re \leq 9.3 \times 10^5$ and $8.1 \times 10^4 \leq Re \leq 9.9 \times 10^5$

The National Water Institute's large-scale stepped spillway models with a slope of $\theta = 26.6°$, 21.8°, 15.9°, 14.6°, and 8.9° were used for the experimental study.

The facility was 12 meters long and was made up of an input tank that continuously delivered an upstream water head. A 0.5 m wide uncontrolled broad-crested weir was used to let water into the experimental test area. The stepped spillway had the following number of steps: a) 10 No steps with a step height of 0.10 m and a step length of 0.20 m; b) 10 No steps with a step height of 0.10 m and a step length of 0.25 m; c) 9 No steps with a step height of 0.10 m and a step length of 0.35 m; d) 13 No steps with a step height of 0.10 m and a step W = 0.52 m was the width of the chute. Perspex was used for the channel walls and PVC for the steps.

A huge upstream intake basin with dimensions of 3.0 m 2.5 m and a depth of 1.6 m provided steady flow rates. A 1.0 m long smooth sidewall convergent with a 4: 1 contraction ratio provided a smooth inflow. A broad-crested weir with a height of 1 m, width of 0.52 m, crest length of 1.01 m 1.01 m, and an upstream rounded corner controlled the flow in the test portion.

An ultrasonic range finder and a sharp-crested weir were used to measure the discharge at the downstream channel's terminus.

The experimental facilities were large scale to minimize scale effects affecting the microscopic air–water flow processes in high-velocity free-surface flows [15]. Scale effect is a term used to describe slight distortions that are introduced by ignoring secondary forces such as viscous forces, surface tension

in stepped spillway models. Viscous forces and surface tension in most open-channel applications are deemed negligible, but in highly air- entrained flows like those expected in stepped spillways, these forces are more dominating and cannot be simply ignored. Scale effects can develop if these factors are ignored, leading to data misinterpretation. Scale effects in modeling stepped spillways have been thoroughly established Boes and Hager [4]. In stepped spillway models, scale effects are most typically linked with scales less than 10: 1.

According to Chanson [10], a model scale of 10: 1 or greater is recommended, and Boes and Hager [3] recommended a minimum Reynolds number of 10^5 and a minimum Weber number of 100. Takahashi et al. [35] urge that Froude, Reynolds, and Morton similarity be satisfied when simulating strongly air entrained flow, but they acknowledge that this can only be done at full scale. Although researchers have not established an agreement on the boundaries to reduce scale effects in physical models of stepped spillways, some information is available. The use of traditional mono-phase flow instrumentation in high-velocity air-water flows is not possible due to the three-dimensional air-water flow with enormous volumes of air-water.

Because substantial quantities of air are entrained at the air-water interface, using a Dall Tube flow meter, or V-notch for flow rates, Prandtl-Pitot for flow velocities, or point gauge for clear water flow depth to get air-water flow attributes is impractical [11, 12].

In stepped spillways, detection invasive probes are widely utilized, and experimental tests with optical fiber probes [1] and conductivity probes [2, 10, 13, 28] have been effective.

Extensive studies were carried out with all of the stepped spillways for a wide variety of discharges 0.018 m^3 /s < Q < 0.117 m^3 /s. Air-water flow studies were carried out with conductivity phase-detection intrusive probes at all step edges downstream of the inception site of air entrainment for all stepped sizes. The sensor diameters of the double-tip conductivity probes were 0.13 mm and 0.25 mm, and they were sampled for 45 seconds at a frequency of 20 kHz per sensor. Typically, the probe was placed at step edges in the air-water flow zone.

The inner diameter of the probe was 0.13 mm for both points, which were separated in the streamwise direction x = 5.1 mm and the transverse direction z = 1 mm.

All measurements lasted 45 seconds at a sampling rate of 20 kHz per probe tip. The conductivity probe's basis is based on the differing resistance of air and water, which provides an immediate voltage signal. A single sensor's signal can be analyzed using a threshold technique to determine the time averaged local air concentration or void fraction C, the number of air-to-water voltage shifts expressed as bubble count rate F, and the air bubble and water droplet chord diameters. The cross-correlation analysis of the data for a double-tip conductivity probe with longitudinal spacing between the two probe sensors yields the local time-averaged interlayer velocity V. Chamani, Chanson [8, 13] provide more information on signal processing techniques

The trials were carried out for a wide variety of discharges at numerous step edges downstream of the free surface aeration inception point.

The discharges had transition and skimming flow rates of $0.035 \leq q_w \leq 0.234$ m^2/s for the spillways with $\theta = 8.9^o$ and $0.02 \leq q_w \leq 0.249$ m^2/s for $\theta = 26.6°$, with Reynolds numbers of $1.4 \times 10^5 \leq Re \leq 9.3 \times 10^5$ and $8.1 \times 10^4 \leq Re \leq 9.9 \times 10^5$, respectively

3. Results

The Developed Models for the Nappe/Transition/Skimming Flow Regime.

The discharges had transition and skimming flow rates of $0.035 \leq q_w \leq 0.234$ m^2/s for the spillways with $\theta = 8.9°$ and $0.02 \leq q_w \leq 0.249$ m^2/s for $\theta = 26.6°$, with Reynolds numbers of $1.4 \times 10^5 \leq Re \leq 9.3 \times 10^5$ and $8.1 \times 10^4 \leq Re \leq 9.9 \times 10^5$, respectively.

The authors then used the developed models, Eq (10) through Eq (19), to predict the rates of energy dissipation and displayed them vis-à-vis the measured data sets in Figure 6 through Figure 15.

$$\Delta H/Hmax = (0.92\ Nh/d_c)^{0.29}\ N^{0.20}\ h^{-0.17}\ \theta^{-0.32} \quad (10)$$

This equation is valid for $\boldsymbol{\theta}$ of 26.6 °, Nh/d_c between 5.0 and 10.0, N between 5 and 20, d_c/h between 0.80 and 3.30, h (cm) between 5 and 10. Spearman coefficient is 0.97.

$$\Delta H/Hmax = (0.28\ Nh/d_c)^{0.29}\ N^{0.20}\ h^{-0.17}\ \theta^{-0.32} \quad (11)$$

This equation is valid for $\boldsymbol{\theta}$ between 21.8 °and 26.6 °, Nh/d_c between 5.0 and 25, N between 5 and 20, d_c/h between 0.80 and 1.85, h (cm) between 5 and 10. Spearman's correlation coefficient is 0.94.

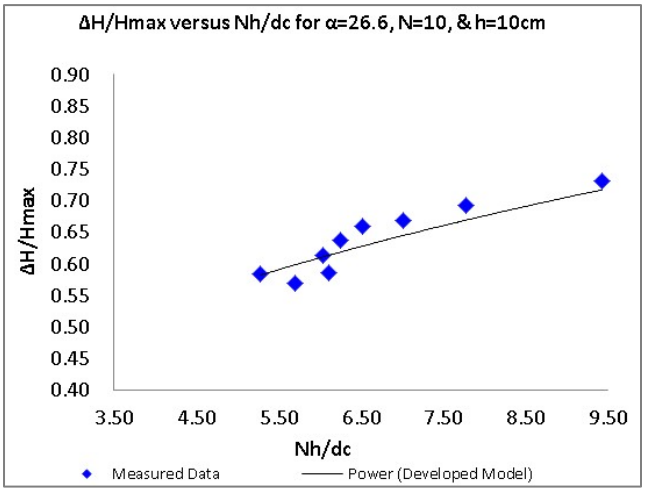

Figure 6. *ΔH/Hmax as a function of Nh/d_c for q_w = (0.073 - 0.249 m^2/s) & Re = (2.92 × 10^5 - 9.96 × 10^5), d_c/h, of (0.80 - 1.85)*

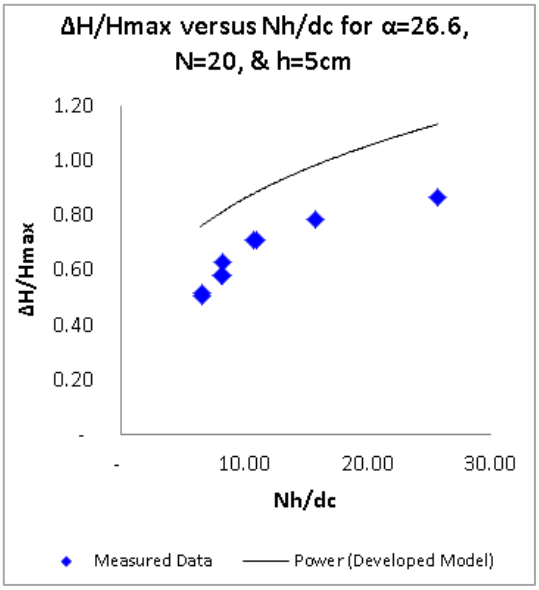

Figure 7. *ΔH/Hmax as a function of Nh/d_c between 4.00 and 10.00, q_w = (0.020 - 0.227) m^2/s & Re = (8.0 × 10^4 - 9.08 × 10^5), flow rate d_c/h, of (0.69 - 3.30). For* θ *= 26.6 °, N = 20, h (cm) = 5.*

$$\Delta H/Hmax=(0.30\ Nh/d_c)^{0.29}\ N^{0.20}\ h^{-0.17}\ \theta^{-0.32} \quad (12)$$

This equation is valid for θ of 21.8 °, Nh/d_c between 5.0 and 11.5, N between 5 and 10, d_c/h between 1.00 and 3.16, h (cm) between 5.0 and 10.0. Spearman's rank correlation coefficient = 0.8.

$$\Delta H/Hmax=(0.25\ Nh/d_c)^{0.29}\ N^{0.20}\ h^{-0.17}\ \theta^{-0.32} \quad (13)$$

This equation is valid for θ between 18.4 °and 21.8 °, Nh/d_c between 5.0 and 12.0, N between 5 and 40, d_c/h and 0.80 and 1.85, h (cm) between 5.0 and 10.0. Spearman's rank correlation coefficient = 0.95.

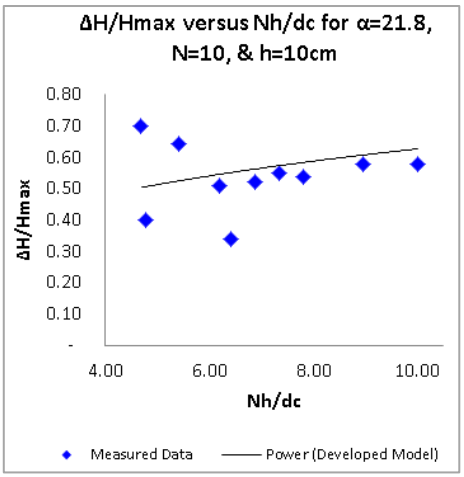

Figure 8. *ΔH/H_{max} as a function of Nh/d_c between 5.00 and 12.00, q_w = (0.095 - 0.180) m^2/s, Re = (3.80 × 10^5 - 7.20 × 10^5), flow rate, d_c/h, of (1.00 - 1.57). For* θ *= 21.8 °, N = 10, h (cm) = 10.*

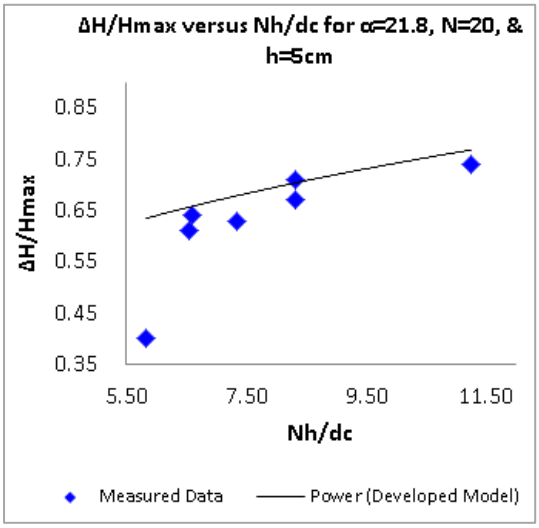

Figure 9. *ΔH/H_{max} as a function of Nh/d_c between 5.50 and 11.00, q_w = (0.059 - 0.158) m^2/s, Re = (2.36 × 10^5 - 6.32 × 10^5), and flow rate, d_c/h, of (0.80 - 1.85). For* θ *= 21.8 °, N = 20, h (cm) = 5.*

$$\Delta H/Hmax=\ (0.1\ Nh/d_c)^{0.29}\ N^{0.20}\ h^{-0.17}\ \theta^{-0.32} \quad (14)$$

This equation is valid for θ between 15.9 °and 18.4 °, Nh/d_c between 21.00 and 30.00, N between 5 and 40, d_c/h between 0.6 and 3.58, h (cm) between 5.0 and 10.0. Spearman's rank correlation coefficient = 1.00.

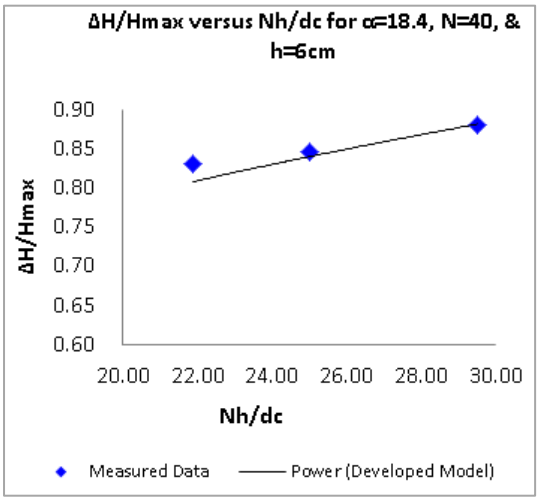

Figure 10. *ΔH/H_{max} as a function of Nh/d_c between 21.00 and 30.00, q_w = (0.059 - 0.158) m^2/s, Re = (2.36 × 10^5 - 6.32 × 10^5), flow rate, d_c/h, of (0.80 - 1.85). For* θ *= 15.9 °, N = 18, h (cm) = 6.*

$$\Delta H/Hmax=(0.12\ Nh/d_c)^{0.29}\ N^{0.20}\ h^{-0.17}\ \theta^{-0.32} \quad (15)$$

This equation is valid for θ of 15.9 °, Nh/d_c between 5.0 and 9.5, N between 5 and 18, d_c/h between 0.6 and 3.2, h (cm) between 5.0 and 10.0. Spearman's rank correlation coefficient =.0.82.

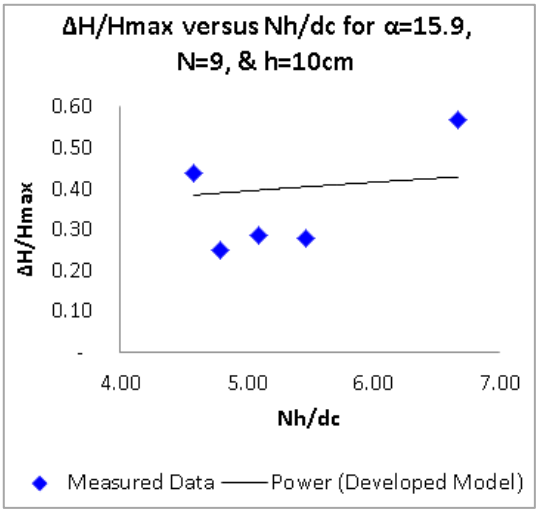

Figure 11. *$\Delta H/H_{max}$ as a function of Nh/d_c for θ = 15.9 °, N = 9, h (cm) = 10, q_w = (0.069 - 0.188) m^2/s, Re = (2.76 × 10^5 - 7.52 × 10^5), d_c/h = (0.78 - 1.53).*

$$\Delta H/Hmax=(0.15\ Nh/d_c)^{0.29}\ N^{0.20}\ h^{-0.17}\ \theta^{-0.32} \quad (16)$$

This equation is valid for θ between 14.6 °and 15.9 °, Nh/d_c between 5.0 and 9.5, N between 5 and 18, d_c/h between 0.60 and 3.20, h (cm) between 5.0 and 10.0. Spearman's rank correlation coefficient = 0.79.

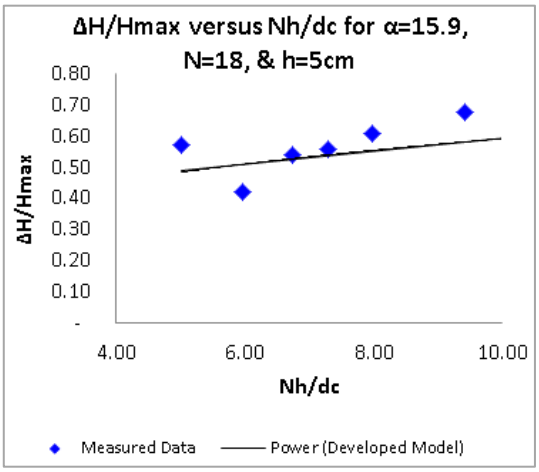

Figure 12. *$\Delta H/H_{max}$ as a function of Nh/d_c between 4.50 and 6.60, q_w = (0.069 - 0.188) m^2/s, Re = (2.76 × 10^5 - 7.52 × 10^5), flow rate, d_c/h, of (0.78 - 1.53). For θ = 15.9 °, N = 9, h (cm) = 1.*

$$\Delta H/Hmax=(0.25\ Nh/d_c)^{0.29}\ N^{0.20}\ h^{-0.17}\ \theta^{-0.32} \quad (17)$$

This equation is valid for θ of 14.6 °, Nh/d_c between 5.0 and 9.5, N between 5 and 26, d_c/h between 1.27 and 3.55, h (cm) between 5.0 and 10.0. Spearman's rank correlation coefficient = 1.00.

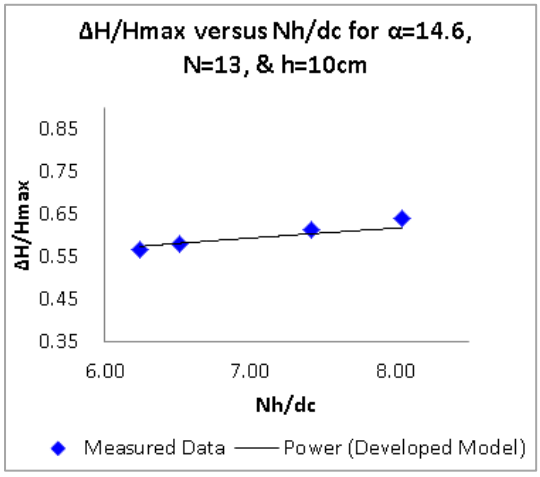

Figure 13. *$\Delta H/H_{max}$ as a function of Nh/d_c between 6.25 and 8.60, q_w = (0.069 - 0.188) m^2/s, Re = (2.76 × 10^5 - 7.52 × 10^5), flow rate, d_c/h, of (0.78 - 1.53). For θ = 14.6 °, N = 13, h (cm) = 10.*

$$\Delta H/Hmax=(0.10\ Nh/d_c)^{0.29}\ N^{0.20}\ h^{-0.17}\ \theta^{-0.32} \quad (18)$$

This equation is valid for θ between 14.6 °and 15.9 °, Nh/d_c between 7.5 and 17.0, N between 5 and 18, d_c/h between 0.60 and 3.20, h (cm) between 5.0 and 10.0. Spearman's rank correlation coefficient = 0.79.

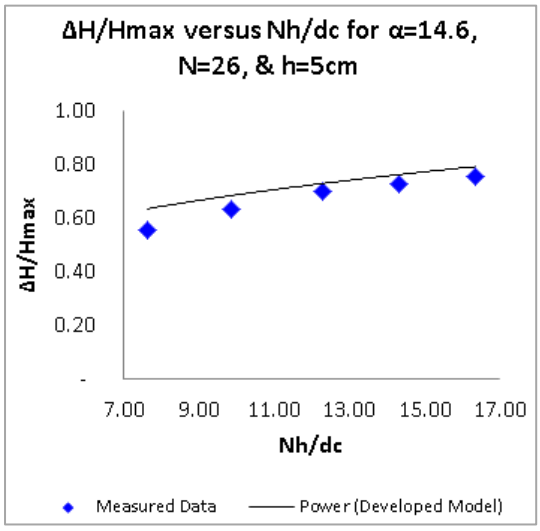

Figure 14. *$\Delta H/H_{max}$ as a function of Nh/d_c between 6.20 and 8.00, q_w = (0.05 - 0.234m^2/s), Re = (2.0 × 10^5 - 9.36 × 10^5), & flow rate, d_c/h, of (1.27 - 3.55). For θ = 14.6 °, N = 26, h (cm) = 5.*

$$\Delta H/H_{max} = (0.18\,Nh/d_c)^{0.29} N^{0.20} h^{-0.17} \theta^{-0.32} \quad (19)$$

This equation is valid for θ between 3.4 °and 8.9 °, Nh/d_c between 8.5 and 14.0, N between 5 and 21, h (cm) between 3.0 and 14.3. Spearman's rank correlation coefficient = (1.00).

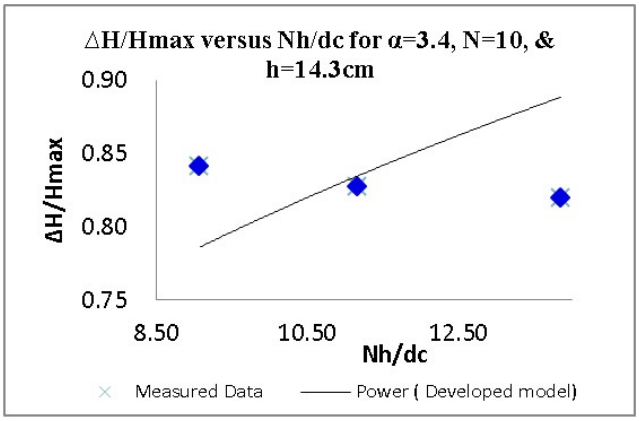

Figure 15. *$\Delta H/H_{max}$ as a function of Nh/d_c between 8.50 and 14.00, q_w = (0.035 - 0.234) m^2/s, Re = (1.40 × 10^5 - 9.36 × 10^5), & flow rate, d_c/h, of (1.0 - 3.55). For θ = 8.9 °, N = 21, h (cm) = 3/6.*

4. Discussions

Figure 6 to Figure 15 depict the energy loss rates as a function of the expression of a dam height divided by the critical depth for the measured data, the developed analytical formulation Eq (10) to Eq (19).

The results from the developed models, Eq (10) to Eq (19), compare well with the measured data sets in terms of energy dissipation, with the Spearman coefficients that range between 0.79 and 1.0.

The models are simple and straightforward to use.

From Figures 6-15 energy losses for a given discharge rise progressively with an increasing dam height, which is consistent with [27].

For all the measured data sets, the dimensionless energy dissipation rates distribution compare well with all the flow regime.

In Figures 9-15, the measured data sets in the nappe flow and skimming flow compare well with the developed data sets from Eq (10) through Eq (19) with the Spearman Correlations from 0.79 to 1.00.

5. Conclusion

The figures depict the energy loss rates as a function of the expression of a dam height divided by the critical depth for the measured data as well as the developed analytical formulation. Both the measured and the estimated data distribution also show same traditional concave shape, which is consistent with [27]. For all the measured data sets, the results from the proposed models, in terms of the dimensionless energy losses rates distribution compare well with the measured data for all the flow regimes with the Spearman Correlations Coefficients that range from 0.79 to 1.00. All the measured data and estimated data are in good agreement. The models are simple and straightforward to use, and they produce accurate results. The energy losses for given discharges rise progressively with increasing dam height, which is consistent with the current findings.

Abbreviations

D_H	Hydraulic Diameter (m)
d_w	Equivalent Clear Water Flow Depth (m)
dc	Critical Flow Depth (m)
g	Gravity Constant (m/s^2)
H	Total Head (m)
H_{dam}	Dam Height (m)
H_{max}	Maximum Upstream Head (m) Above Chute Toe Hmax = H_{dam} + 3/2 ×dc
H_{res}	Residual Head (m)
h	Vertical Step Height (m)
I	Horizontal Step Length (m)
q_w	Water Discharge Per Unit Width ($m^{2/}s$)
Re	Reynolds Number Defined in Terms of the Hydraulic Diameter: Re = ρw×Uw×DH/μw
Uw	Mean Flow Velocity (m/s): Uw = qw/d
Uw	Average Mean Flow Velocity (m/s) for Stepped Spillway
W	Channel Width (m)
Y_{90}	Characteristic Depth (m) Where the Void Fraction Is -90%
D	Distance (m) Measured Normal to the Invert (or Channel Bed)
ΔH	Total Head Loss (m): ΔH = Hmax – Hres
θ	Angle Between Pseudo-bottom Formed by the Step Edges and the Horizontal
c	Critical Flow Conditions
max	Maximum Value
mean	Mean Signal Component
w	Water Properties

Acknowledgments

I acknowledge the fruitful discussions and contributions of Prof Hubert Chanson of the Department of Civil Engineering, The University of Queensland, Brisbane QLD 4072, Australia.

Author Contributions

Okechukwu Ozueigbo: Conceptualization, Data curation, Formal Analysis, Investigation, Resources, Software

Jonah Agunwamba: Conceptualization, Investigation, Project administration, Resources, Supervision, Validation

Conflicts of Interest

The authors declare no conflicts of interest.

References

[1] Beitz E, Lawless M. Hydraulic Model Study for darn on GHFL 3791 lsaac River al Burton Gorge. Water Resources Commission Report, Ref. No. REP/24.1, Sept., Brisbane, Australia; 1992.

[2] Bindo M, Gautier J, Lacrotx F. The Stepped Spillway of: Vl"Bah Darn. lntl Water Power and Dam Construction. 1993; 1-5(1): 35-36.

[3] Boes R, Hager WH. Two-phase flow characteristics of stepped spillways. J. Hydraul. Eng. ASCE. 2003a; 129(9): 661-670.

[4] Boes RM. Scale effects in modeling two-phase stepped spillway flow. In Proc. Intl. Workshop on Hydraulics of Stepped Spillways, Minor HE and Hager WH, eds. Steenwijk, The Netherlands: A. A. Balkema. 2000: 53-60.

[5] Bung D, Schlenkhoff A. Prediction of oxygen transfer in self-aerated skimming flow on embankment stepped spillways, 33rd IAHR World Congress. Vancouver, Canada 123 Author's personal copy Environ Fluid Mech; 2009.

[6] Bung DB. Zur selbstbelüfteten Gerinneströmung auf Kaskaden mit gemäßigter Neigung. PhD Thesis, Lehr- und Forschungsgebiet Wasserwirtschaft und Wasserbau, Bergische Universitaet Wuppertal, Germany (in German); 2009.

[7] Carosi G, Chanson H. Air-water time and length scales in skimming flow on a stepped spillway. Application to the spray characterisation. Report No. CH59/06, Division of Civil Engineering, the University of Queensland, Brisbane, Australia, July; 2006.

[8] Chamani R, Rajaratnam N. Jet Flow on Stepped Spillways. J. Hydraul. Engg. ASCE 1994; 120(2): 254–259.

[9] Chanson H, Carosi G. Advanced post-processing and correlation analyses in high-velocity air– water flows. Environ Fluid Mech. 2007; 7(6): 495–508.

[10] Chanson H, Toombes L. Air–water flows down stepped chutes: turbulence and flow structure observations. Int J Multiph Flow. 2002a; 28(11): 1737–1761.

[11] Chanson H, Toombes L. Energy dissipation and air entrainment in stepped storm waterway: experimental study. J Irrig Drain Eng ASCE. 2002b; 128(5): 305–315.

[12] Chanson H, Toombes L. Supercritical Flow at an Abrupt Drop: Flow Patterns and Aeration". Can. J. Civil Eng. 1998; 25(5): 956–966.

[13] Chanson H. The hydraulics of stepped chutes and spillways. Balkema, Lisse. 2001: 418.

[14] Chanson H. Air bubble entrainment in open channels. Flow structure and bubble size distributions. Int J Multiph Flow. 1997a; 23(1): 193–203.

[15] Chanson H. Air–water flow measurements with intrusive phase-detection probes. Can we improve their interpretation? J Hydraul Eng ASCE. 2002; 128(3): 252–255.

[16] Chanson H. Measuring air–water interface area in supercritical open channel flow. Water Res. 1997b; 31(6): 1414–1420.

[17] Chanson, H. 1994a. Hydraulics of skimming flows over stepped channels and spillways. Journal of Hydraulic Research, 32(3): 445-460.

[18] Chanson, H. 1994b. Comparison of energy dissipation between nappe and skimming flow regimes on stepped chutes. Journal of Hydraulic Research, 32(2): 213-218.

[19] Degouite G, Peyras L, Royet P. Skimming Flow in Stepped Spillways - Discussion. Jl of Hyd. Engrg., ASCE. 1992; 118(1): 111-114.

[20] Essery ITS, Horner MW. The hydraulic design of stepped spillways, Rep. 33, Construction Industry Research and Information Assoc., London, U. K; 1971.

[21] Felder S, Chanson H. Air–water flow properties in step cavity down a stepped chute. Int J Multiph Flow. 2011; 37(7): 732–745.

[22] Felder S, Chanson H. Energy dissipation and flow resistance on flat slope stepped spillways. 5th IAHR International Symposium on Hydraulic Structures, Brisbane, Australia, 25-27 June 2014. Brisbane, Australia: The University of Queensland; 2014.

[23] Felder S, Chanson H. Energy dissipation, flow resistance and gas-liquid interfacial area in skimming flows on moderate-slope stepped spillways. Environ Fluid Mech. 2009a; 9(4): 427–441.

[24] Felder S, Chanson H. Turbulence, dynamic similarity and scale effects in high-velocity free surface flows above a stepped chute. Exp Fluids. 2009b; 47(1): 1–18.

[25] Felder S. Air–water flow properties on stepped spillways for embankment dams: aeration, energy dissipation and turbulence on uniform, non-uniform and pooled stepped chutes. PhD Thesis, The University of Queensland, Australia; 2013.

[26] Gonzalez CA. An experimental study of free-surface aeration on embankment stepped chutes. PhD Thesis, Department of Civil Engineering, The University of Queensland, Brisbane, Australia; 2005.

[27] Guenther P, Felder S, Chanson H. Flow aeration, cavity processes and energy dissipation on flat and pooled stepped spillways for embankments. Environ Fluid Mech. 2013; 13(5): 503–525.

[28] Ohtsu I, Yasuda Y, Takahashi M (2004) Flow characteristics of skimming flows in stepped channels. J Hydraulic Eng ASCE 130(9): 860–869.

[29] Ozueigbo, O, Agunwamba J, New Equations for Energy Dissipation down a Stepped Spillway. Journal of Engineering Research and Reports 23(4): 1-14, 2022; Article no. JERR. 90654 ISSN: 2582-2926, https://doi.org/10.9734/JERR/2022/v23i417602

[30] Peyras L, Royet P, Degoutte G. Flow and Energy Dissipation over Stepped Gabion Weirs." Jl of Hyd. Engrg. ASCE. 1992; 118(5): 707-717.

[31] Rajaratnam N. Skimming flow in stepped spillways. J. Hydr. Engrg., ASCE. 1990; 116(4): 587-591.

[32] Sorensen, RM. 1985. Stepped spillway hydraulic model investigation. Journal of Hydraulic Engineering, 111(12): 1461-1472.

[33] Stefan Felder, Hubert Chanson (2014). Aeration and air–water mass transfer on stepped chutes with embankment dam slopes, Environ Fluid Mech; 2014. https://doi.org/10.1007/s10652-014-9376-x

[34] Stephenson, D. (1991). "Energy Dissipation down Stepped Spillways." International Water Power & Dam Construction, Sept., pp. 27-30.

[35] Takahashi, M., Yasuda, Y., and Ohtsu, I. (2008). Flow Patterns and Energy Dissipation over Various Stepped Chutes. Discussion. Jl of Irrigation and Drainage Engineering, ASCE, Vol. 134, No. 1, pp. 114-116.

Research Field

Okechukwu Ozueigbo: Civil Engineering, Water Resources, Environmental Analysis, Soil Erosion

Jonah Agunwamba: Civil Engineering, Water Resource, Environmental Analysis, Soil Erosion